



Recovery of forest carbon density and carbon storage in a soil-degraded landscape in southeastern China

Kaijian Xu¹ · Chung-Te Chang^{2,3} · Qingjiu Tian¹ · Hongda Zeng⁴ · Jinsheng Xie⁴

Received: 10 September 2018 / Revised: 27 January 2019 / Accepted: 1 February 2019 / Published online: 11 February 2019
© Springer-Verlag GmbH Germany, part of Springer Nature 2019

Abstract

Adaptive managements on susceptible forested regions not only benefit forest recovery, but also help to improve the stability of soil-degraded area and carbon (C) sequestration. The gain of afforestation on C sink has not been addressed clearly especially in tropical and subtropical regions that will be critical in an era of global warming. Based on the Landsat satellite images, in situ forest survey and archives, we analyzed the spatiotemporal patterns of C density and storage in a typical soil–water conservation area in Changting county in southeastern China, dominated by the pioneer tree *Pinus massoniana* forest. The results showed that the C density (storage) increased significantly from 20.14 Mg C ha⁻¹ (0.38 Tg C) in 1981 to 43.57 Mg C ha⁻¹ (1.98 Tg C) in 2015 ($p < 0.05$) and proved the success of ecological management adopted considering the interactions between local residential livelihoods and the features of local forest ecosystem. In addition, the differences of C density and storage across elevational and slope gradients also narrowed over the past 35 years. The landscape also gradually shifted from lower C density to higher C density conditions based on the landscape metrics. The ecological-dominated approaches should be put in a high priority for the issue of C sequestration especially in a changing climate.

Keywords Red soil eroded area · Ecological restoration · *Pinus massoniana* · Forest carbon density · Carbon storage · Ecological governance

Introduction

Forests are the largest terrestrial carbon (C) pool which have stored more than 76% of aboveground organic C of terrestrial biosphere, and as such are critical in mitigating climate change (Dixon et al. 1994; Fang 2000; Houghton et al. 2007; Canadell and Raupach 2008; Pan et al. 2011). A

better comprehension of the spatiotemporal patterns of forest aboveground C density (ACD; the carbon stored in the aboveground tissues of vegetation, commonly expressed in units of Mg C ha⁻¹) and its C storage (total carbon storage in a specific region) is important for the efficiency of forest management practices and regional efforts on C budget (Zhao and Zhou 2006; Asner et al. 2012; Wang et al. 2016). Globally, the long-term estimations (1980–2002) suggested that the climate changes and rising CO₂ concentration had forced the land C sink (1.6–2.2 Pg C yr⁻¹) compared to C emissions (1.0–1.2 g C yr⁻¹) except for tropical regions where the net C balance was neutral due to the rapid change of land use (Piao et al. 2009). Because the loss of C storage from land use changes is rapid than recovery, the land cover changes and management are responsible for future C emissions (Houghton 2003; Jain and Yang 2005). In many marginal and fragile regions such as mountainous and hilly ecosystems with steep terrain, the forests are regularly harvested for firewood and for livelihood which will easily lead to soil erosion and a significant loss of C (Nave et al. 2010; Persha et al. 2011; Mekonnen et al. 2014). The soil loss and the consequent fertility degradation is undoubtedly a serious

Communicated by Agustín Merino.

✉ Chung-Te Chang
changchuante@gmail.com

✉ Qingjiu Tian
tianqj@nju.edu.cn

¹ International Institute for Earth System Science, Nanjing University, Nanjing 210023, China

² Department of Life Science, Tunghai University, Taichung 40704, Taiwan

³ Center for Ecology and Environment, Tunghai University, Taichung 40704, Taiwan

⁴ College of Geographical Sciences, Fujian Normal University, Fuzhou 350007, China

threat to environmental sustainability and economy on which local population depends. It is also a conundrum for local people and government to strike a balance between environmental protection and economic demands (Wang et al. 2016; Das et al. 2017).

China is one of the countries suffering from serious soil erosion, with approximately 3.5 million km² or 37% of the land area of China is designated as soil erosion area (Zhao et al. 2013; Wang et al. 2016). The average annual loss of soil erosion could account for 20% of global soil erosion which results in 0.6% economic loss of the annual GDP of China (Hao et al. 2004; Sun 2011). Soil erosion not only distributed on arid and semi-arid regions but also the subtropical China with humid monsoon climate. To mitigate the environmental degradation, China has carried out a series of national conservation programs since 1990s such as the Natural Forest Conservation Program (NFCP). The NFCP plans to recover natural forests while meet the internal demand for timber from the plantations by 2050 (Liu et al. 2008), as well as many regional projects (Louks et al. 2001; Zhang 2006). Over the past two decades, many studies have investigated the efficiency and benefits of afforestation and plantation on aboveground C storage with field forest inventory in the inland of northern China (Zhang et al. 2009; Liu et al. 2011; Zhao et al. 2014; Zeng et al. 2014; Wang et al. 2015) and combined satellite data in broader scale estimations (Piao et al. 2005; Tan et al. 2007). A national measurement of in situ ACD over the past five decades and showed that there were an increasing trends of C density for plantations from 15.3 Mg C ha⁻¹ in 1973 to 31.1 Mg C ha⁻¹ in 1998, while the C density for natural and secondary forests maintained in a stable condition (49 Mg C ha⁻¹) between 1979 and 1998 (Fang and Chen 2001). However, the spatiotemporal complete estimations on forest ACD in a larger scale are unavailable except for northeast China (Tan et al. 2007) and southwest China (Zhang et al. 2013). The forest biomass C in highly inhabited coastal southeast China with heavily anthropogenic disturbances are much less understood. The analysis of spatiotemporal patterns of C storage is critical for forest management in the tropical and subtropical region not only the potential of forest growth and recovery is increasing but also the implication of C cycle in developing countries (Cao et al. 2009). This information is fundamental to meet the requirement of Kyoto Protocol on C trading.

Compared to field survey, satellite imagery is a cost-effective approach to analyze the changes on land surface over a broad scale (Nemani et al. 2013). The integration of remotely sensed datasets with in situ observations can clearly reveal spatiotemporal patterns of estimation of forest biomass C storages (Myneni et al. 2001; Dong et al. 2003; Goetz and Dubayah 2011; Dubayah et al. 2015). Saatchi et al. (2011) mapped the biomass C storages of forests of tropical forests over three continents with satellite images and in situ plot

inventory, which aimed to produce a more robust estimation of historic emissions and to assist countries reducing deforestation and degradation at regional scales. Madugundu et al. (2008) indicated that the ground-based measurements such as leaf area index (LAI) and biomass of tropical broad leaf forests can be well estimated by normalized difference vegetation index (NDVI) in Western Ghats of Karnataka, India using IRS P6 LISS-IV multispectral images. Tan et al. (2007) utilized forest inventory and the National Oceanic and Atmospheric Administration's Advanced Very High Resolution Radiometer (NOAA AVHRR) NDVI datasets during 1982–1999 to estimate forest biomass C storage in northeast China, showing that the climate warming might be the factor for the increase of C storage but deforestation or afforestation contributed the annual variations of C storage. Utilizing Landsat TM images and forest inventory plot data to investigate the impacts of urban sprawl on forest C storage changes in Xiamen, southeast China, Ren et al. (2012) reported that human disturbance dominated the variations of C density and storage of forest patches.

Changting county, a mountainous region in subtropical southeast China, had suffered severe soil loss over the past half century in which the Hetian basin was the typical area (Xie et al. 2013). The highly weathered and loose structure of red soil, steep terrain and the heavy rainfall storms led to significant sediment yields and soil erosion (Zhu 2013). The long-term poverty of local people accelerated the deterioration of environment due to over harvest of timber, excessive tillage and subsequent loss of soil fertility during 1980s (Xie et al. 2004; Wang et al. 2012). In 1983, the total soil erosion area in Hetian basin was 15,840 ha, accounting for 45% of the total region (Wu 2011), and the sediment yields from soil erosion reached up to 5000–12,000 t km⁻² (Yang et al. 2005a). Since then the government initiated the long-term plan of ecological restoration and *Pinus massoniana* was selected as a suitable tree species for afforestation on severely degraded lands in subtropical China due to its fast growth and adaptability to dry and infertile soils (Yang et al. 2005b). The afforestation gradually increased vegetation coverage, accumulated litter-fall mass, constructed root networks, and improved soil physiochemical properties, which in turn reduced runoff and soil loss (Gao and Liu 1992; Hou et al. 1996; Li and Shao 2006). The comparisons of site factors on productivity of 5-year-old *Pinus massoniana* forest indicated that the productivity of forest at downslope (1.70 t ha⁻¹ yr⁻¹) was higher than that at upslope (0.97 t ha⁻¹ yr⁻¹) (Huang 2002). The tree-ring analysis of *Pinus massoniana* forest during 1945 and 2009 demonstrated that the temperature ≥ 10 °C during the growing season and soil water availability would promote the growth and consequent productivity (Cheng et al. 2011; Feng et al. 2011). There was a long

history of anthropogenic interventions and management in Changting county at southwest Fujian (Cao et al. 2009; Wang et al. 2011a, 2016), but no effort conducted to estimate forest C density and storage on landscape using time-series remotely sensed data.

Therefore, this study aims to quantify the spatiotemporal patterns of forest C density and storage in a typical soil-degraded region between 1981 and 2015. The objectives of this study are to (1) map the spatiotemporal patterns of C density and storage over the past 35 years; (2) analyze if the forest C density and storage in red soil-degraded region recover effectively with long-term ecological governance; and (3) further examine the landscape structure of C density using landscape metrics.

Materials and methods

Study area

The study region, situated within Changting county, is located at southwestern Fujian province of southeast China, and is a key water and soil erosion control zone with 870.8 km² (25°40' N, 116°40' E; Fig. 1). The topography is featured as a basin (Hetian basin) surrounded by hills and mountains ranging from 225 to 1084 m a.s.l. (Fig. 1b and c). The climate in the region is typical humid subtropical monsoon climate, and the mean annual temperature is 18.6 °C with lowest 8.3 °C in January and highest 27.1 °C in July. The mean annual precipitation is 1714 mm with 70–80% concentrating in growing summer (May to September) and

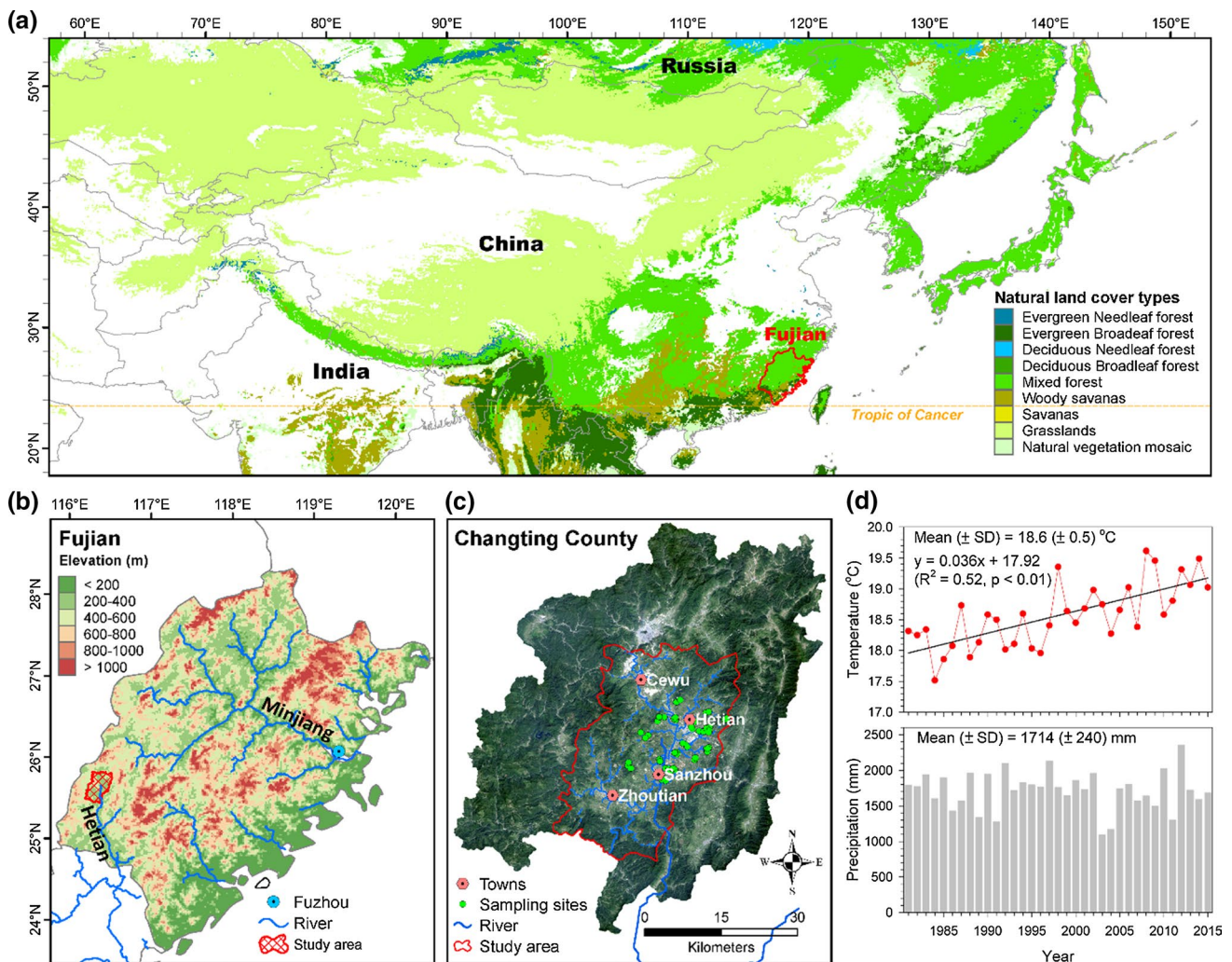


Fig. 1 The geographical map of Fujian province with vegetation types in China (a), the location of Changting county, the elevational patterns and the river system in Fujian (b), study area (red boundary) and sampling plots (green dots) in Changting county with a true-color

OLI image in 2015 November in background (c), and the trends of annual mean temperature and annual precipitation during 1981 and 2015 (d). (Color figure online)

the winter is a relative dry period (Zhao et al. 2016). There is a significant elevating trend of annual mean temperature in 1 °C during 1981 and 2015 ($R^2=0.52$, $p<0.01$), but not for annual precipitation (Fig. 1d). Hetian basin is a region characterized with serious soil erosion in Fujian, also called Red Desert in China (Cao et al. 2009). The vegetation types were dominated by the *Pinus massoniana* afforestation, which accounted for more than 82% of forestland in the study area and the remained area were covered by a shrub species, *Dicranopteris dichotoma Bernh* (Zeng et al. 2014).

The Red Desert was exacerbated by deforestation due to overpopulation and the extreme rainfall events, especially the summer irregular intense rainfalls over the past hundred years, which also created an ecological barrier in southern China (Zhao et al. 2006). To mitigate the land degradation, the Hetian experimental zone was initiated since 1940 for soil and water loss control. In 1981–1989, Fujian provincial government laid out large-scale projects (first project) for water and soil conservation focused on the four hotspot areas (towns) of erosion (Cewu, Hetian, Sanzhou, and Zhoutian; Fig. 1c) in which accounted for 52% and 93% of soil erosion and collapse gully area of the total county, respectively (Luo 1994). The major works in the first project included selecting tree species of plantation which were resistant to drought and infertile soil, and some fast-growing grasses to increase vegetation coverage both were beneficial for the environmental stable. The tree harvesting and grazing of domestic livestock were restricted during this period (Cao et al. 2009).

However, the implementation of project was suspended after 1990 (Intermission) which interrupted the support of ecological management and the recovery of forest cover and C storage (Xie et al. 2013; Xu et al. 2016b). In order to improve ecological restoration and economic condition, the following environmental policy was carried out since 2000 (second project, Cao et al. 2009). The strategies adapted during the second project included closing hillsides for afforestation, planting trees along the elevational contour, forest fertilization, planting fruit trees and irrigating on the grass belts between forests. Furthermore, the authority of Fujian province provided a compensation of 10 million RMB annually (equal to 1.55 million US dollar in 2000) to four towns, Cewu, Hetian, Sanzhou, and Zhuotian, as living subsidies

to farmers and residents to stop timber harvest for firewood and electricity infrastructure were substitute for timber burning. The government further encouraged the farmers to plant trees by providing a compensation of 1500 RMB per hectare (Cao et al. 2009).

Remotely sensed data and preprocessing

The Landsat images provide a long-term continuous earth observations > 40 years since 1970s with 30–60 m resolution datasets, which is powerful to exhibit the land surface changes over time. In this study, seven images (raw 121 and column 42) during September and December in 1981, 1989, 1995, 2000, 2006, 2010, and 2015, respectively, in which the cloud over were < 0.1%, were acquired from USGS (Table 1; <http://glovis.usgs.gov/>). The 2015 image was georeferenced using orbital parameters and ground reference points geolocated with a Global Positioning System (GPS) of which error was less than 1 m (Fig. 2). Then, it was used as a reference image to co-register the others, using an image-to-image registration with a second-order polynomial transformation and nearest neighbor resampling, by at least 90 ground control points (GCPs), to reach the lowest root mean square error (RMSE) less than 0.35 pixels (Xu et al. 2017).

The atmospheric effect was corrected by surface reflectance of image applying illumination and atmospheric correction model (IACM; Homer et al. 2003), which was confirmed to significantly improve the image quality (Ramsey et al. 2004; Xu 2008). In order to further reduce the influences of temporal varieties of surface radiation and the differences of meteorological condition (Sehott et al. 1988), we selected pseudo-invariant feature points (such as house-top, highway, and crossover of major roads) of the reference image and established the regression models to finish associated radiometric normalization in all images (Xu et al. 2017). The spectral radiometric correction was based upon the field measurements of various vegetation types from normal to pathological conditions using a ground ASD spectrometer (Analytical Spectral Devices, Boulder, Colorado, CO, USA) and their relationships to spectral information derived from images (Xu et al. 2017). All these preprocessing processes were all conducted in ENVI (Environment for

Table 1 The basic information of Landsat images used

Acquisition data	Raw/column	Earth-sun distance	Solar elevation (°)	Solar azimuth (°)
1981/12/8	121/42	0.98506	32.680515	145.193694
1989/11/20	121/42	0.98809	36.710122	146.141639
1995/12/7	121/42	0.98519	30.541501	141.493698
2000/11/2	121/42	0.99228	42.931754	147.354712
2006/11/3	121/42	0.99202	44.517932	152.011884
2010/10/29	121/42	0.99339	45.439764	149.559697
2015/11/28	121/42	0.98358	39.031874	156.029355

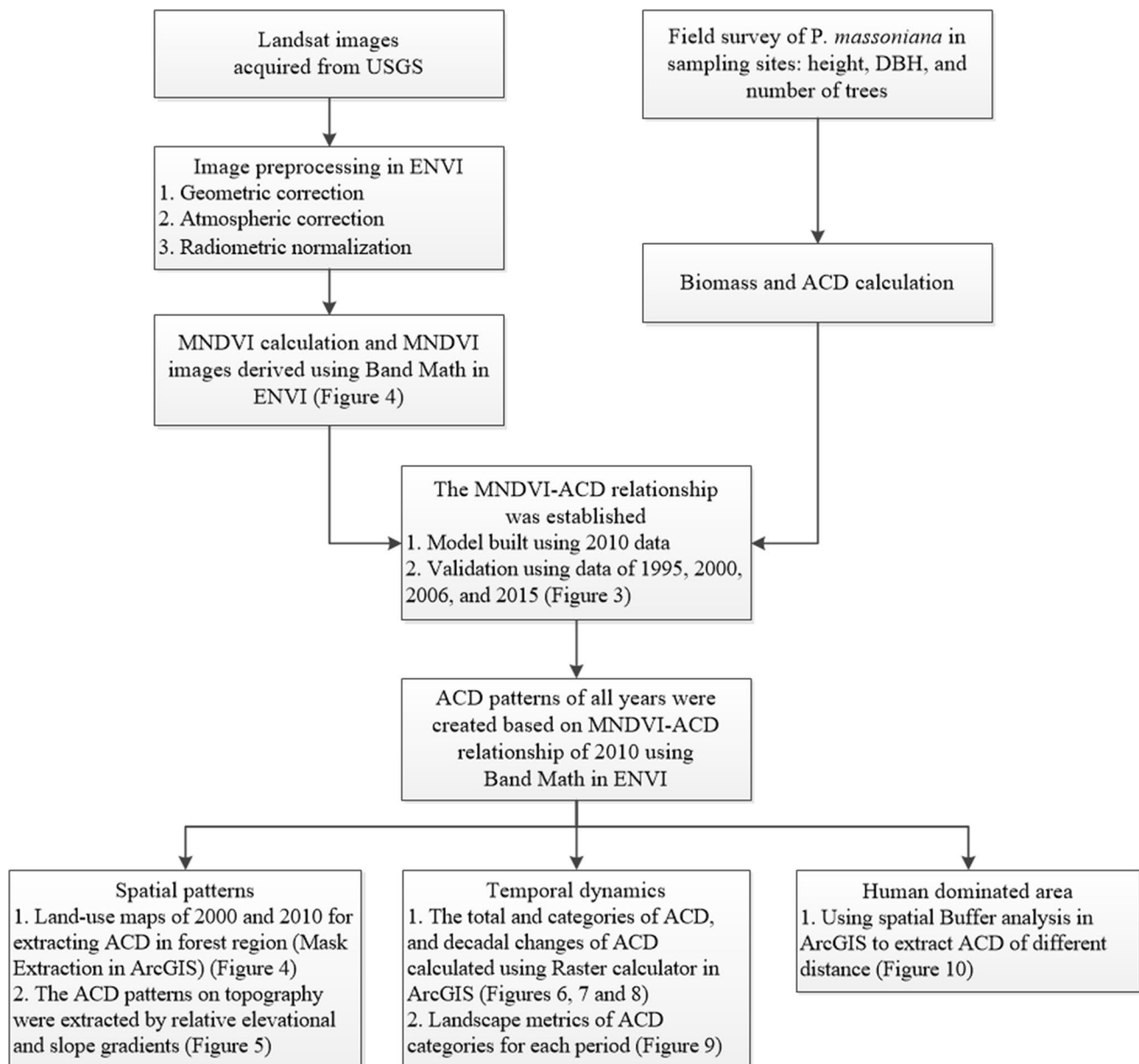


Fig. 2 The working flow of major images and data processing, calculation, and analysis in ENVI and ArcGIS software

Visualizing Images software, version 5.1, Research Systems Inc., Boulder, CO, USA) (Fig. 2).

Data of forest inventory

In November 2010, in total of 50 sampling sites (20×20 m plots) were selected for complete enumeration of *Pinus massoniana* forest within the study area which was conducted by county authority (Fig. 1c), information including number of trees, coordinate, DBH (diameter at breast height), height, and basal area. The average slope of plots changed from flat (3°) to steep landscape (36°), and included major aspects

such as north, south, east, west, southwest, southeast, northwest, and northeast. The stand age varied from 21 to 35 year and the tree density ranged from 1400 to 3400 trees ha^{-1} , and the understory vegetation coverage comprised from 30 to 100%. The tree height and DBH ranged from 4 m and 5.6 cm to 17 m and 20.3 cm, respectively, of sampling sites. The data in 2010 was used to build the relationship between measured ACD and vegetation index derived from satellite images as descriptions in next two sections. Then, the survey of *Pinus massoniana* forest plots in 1995 ($n=9$), 2000 ($n=9$), 2006 ($n=9$), and 2015 ($n=14$) in study region conducted by Changting county Forestry Bureau (<http://www>.

ctlyj.com) were all together utilized to validate the regression model established based on 2010 data (Fig. 2).

Maps of *Pinus massoniana* forest and topographic information

The distribution map of *Pinus massoniana* forest in 2006 was generated based on the forest inventory from Changting county Forestry Bureau, from which the maps of *Pinus massoniana* forest in 1981, 1989, 1995, 2000, and 2010 were also created separately by recalculating the stand age referred to the map of 2006. The *Pinus massoniana* forest map in 2015 was created based on the forest survey in 2013 (Fig. 2). The accuracies of classification were > 94% at least for all maps, indicating that the results were reliable.

In addition, to understand the dynamics of spatial pattern ACD of *Pinus massoniana* forest away from inhabited regions, nine buffers (distances) (50 m, 100 m, 200 m, 400 m, 600 m, 800 m, 1000 m, 1200 m, and 1500 m) outside of residential patches were created in GIS and was used to reveal the patterns of ACD with time (Sanchez-Azofeizi et al. 2009). The different regions of distances (buffers) were generated using the buffer analysis in analysis tool of ArcGIS, the polygons of different distances were utilized to extract the ACD images using the mask analysis and to calculate the ACD values of different periods using raster calculator in spatial analyst tool of ArcGIS (Fig. 2). To avoid the influences of buildup areas on calculations, the land use maps of 2000 and 2010, acquired from Land and Resources Bureau of Changting county, were applied for extracting forest region for first four periods (1981, 1989, 1995, and 2000) and later three periods (2006, 2010, and 2015), respectively. The landscape patterns of forest C density and storage along the elevational gradients (< 400, 400–600, 600–800, and > 800 m) and slope gradients (< 5°, 5–15°, 15–25°, 25–35°, and > 35°) were based on the 30 m resolution digital elevation model (DEM; Fig. 1b). The extent of forest regions and their topographical distribution of ACD based upon elevational and slope ranges were conducted using the mask analysis in spatial analyst tool of ArcGIS (Fig. 2).

Aboveground carbon density (ACD) calculation

The biomass of individual *Pinus massoniana* tree (diameter > 3 cm, in total of 70,708 trees) in each of 50 sampling sites (1400–3400 trees ha⁻¹) in the region was calculated based on the allometric relationship of *Pinus massoniana* following Eq. (1) (Han et al. 2013).

$$Bs = 0.0292 \times (\text{Diameter}^2 \times \text{Height}) + 3.505 \quad (1)$$

where the Bs is the biomass of individual *Pinus massoniana* tree with diameter > 3 cm. The vegetation C storage

of each sampling site was calculated by multiplying the all trees' biomass and C content of biomass (Olson et al. 1983), 53.99%, which was the arithmetic weighted average of *Pinus massoniana* as suggested (Han et al. 2013). Then, the ACD (Mg C ha⁻¹) of each sampling site can be derived from the sum of all trees' biomass divided by area.

In order to estimate the spatial patterns of forest C storage for study region, the relationship between modified normalized difference vegetation index (MNDVI) derived from Landsat images and the in situ measured ACD ($n = 50$) in 2010 based on biomass empirical statistical models was built (Fig. 2). The MNDVI instead of NDVI was used here to avoid overestimation of forest C storage by the effects of the understory vegetation (Zeng et al. 2014). Because the reflectance of canopy forest (*Pinus massoniana*) and understory can be well separated by integrating with SWIR (short wave infrared) band (Zeng et al. 2014). The MNDVI can be calculated as Eq. (2):

$$\text{MNDVI} = \frac{(\text{NIR} - R) \times (\text{SWIR}_{\max} - \text{SWIR})}{(\text{NIR} + R) \times (\text{SWIR}_{\max} - \text{SWIR}_{\min})} \quad (2)$$

$$\text{ACD} = 1.243 \times e^{8.399\text{MNDVI}} \quad (3)$$

where the R and NIR are the surface reflectance of Red and near infrared (NIR) bands, respectively. SWIR_{\max} and SWIR_{\min} are the maximum and minimum SWIR values in the image of the area in analysis. Finally, a close relationship between ACD and MNDVI ($R^2 = 0.87$, $p < 0.001$) of *Pinus massoniana* forest in the study area was established (Eq. (3), Fig. 3a), which performed much better than previous study (Tan et al. 2007). The MNDVI and ACD images can be created using Band Math tool in ENVI using Eqs. (2), and (3), respectively, for difference periods (Figs. 2, 3 and 4).

The relative deviation (RE, Eq. 4) and root mean square error (RMSE, Eq. 5) were used to verify the prediction accuracy of validation data of 1995, 2000, 2006, and 2015 (Huang et al. 2013).

$$\text{RE} = \frac{1}{n} \sum_{i=1}^n \left(\frac{C_{\text{Pre},i} - C_{\text{Mea},i}}{C_{\text{Mea},i}} \right) \times 100\% \quad (4)$$

$$\text{RMSE} = \sqrt{\frac{\sum_{i=1}^n (C_{\text{Pre},i} - C_{\text{Mea},i})^2}{n}} \quad (5)$$

where $C_{\text{Pre},i}$ and $C_{\text{Mea},i}$ are the predicted and measured ACD of *Pinus massoniana* forest, and n is the sample size. The predicted and measured ACD showed a close relationship with a regression slope equal to 1 ($y = -0.35 + 1.023x$, $R^2 = 0.96$, $p < 0.001$; Fig. 3b), indicating the well performance of estimation with low RE (9.27%) and RMSE (6.24 Mg ha⁻¹, Fig. 3b).

Fig. 3 The relationships between MNDVI and measured aboveground carbon density (ACD) in 2010 (a), and validation between predicted ACD and measured ACD based on the data of 1995, 2000, 2006, and 2015 (b). The gray dash line indicates 1: 1 line

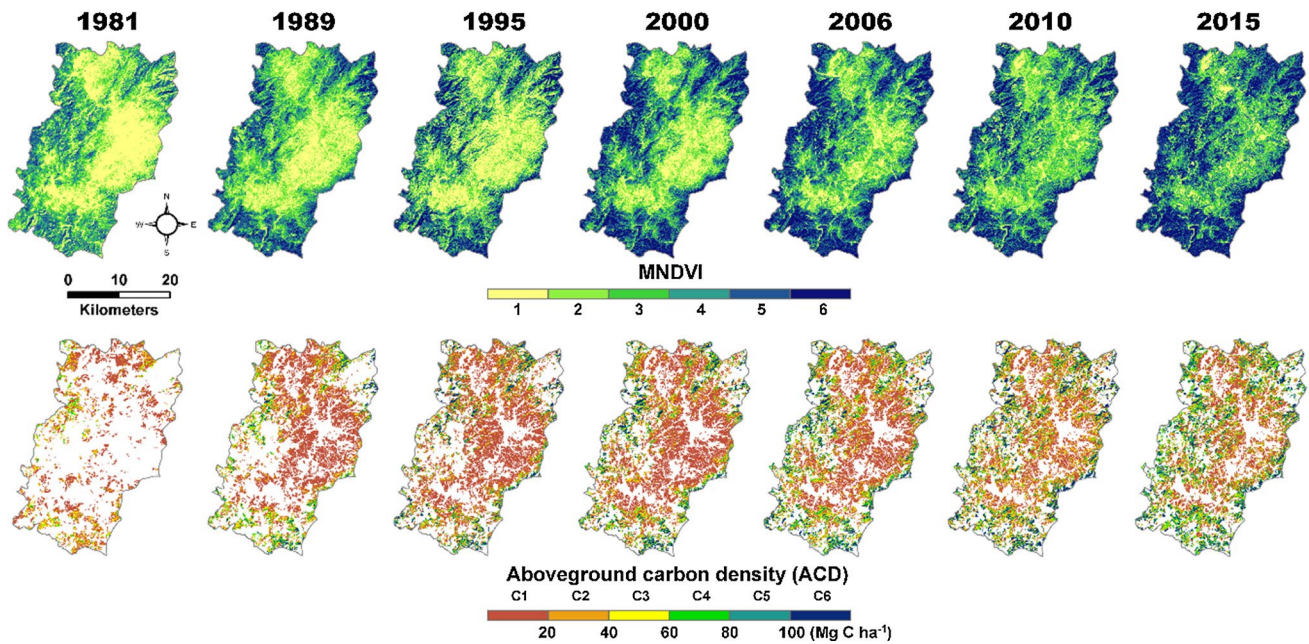
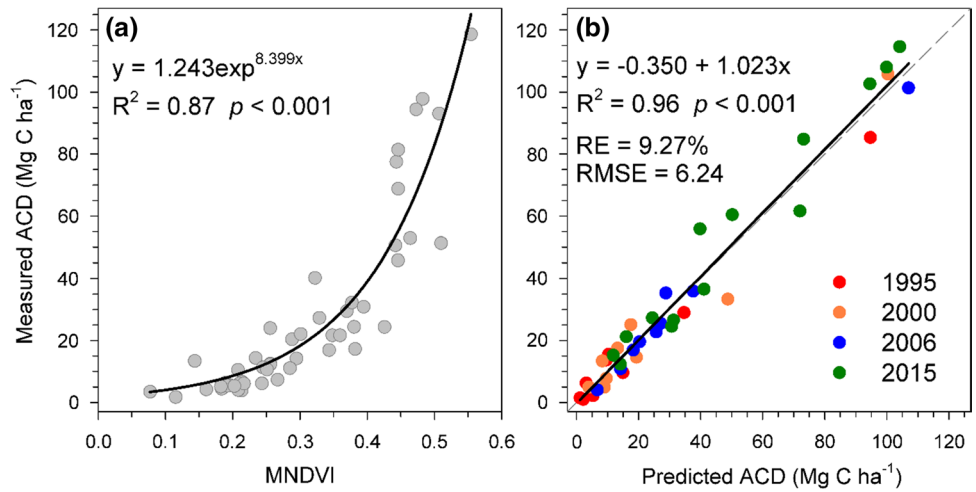


Fig. 4 The spatiotemporal patterns of MNDVI and the aboveground carbon density (ACD) of *Pinus massoniana* forest in the study area for 7 years (1981, 1989, 1995, 2000, 2006, 2010 and 2015)

The trends of annual C density and storage, and their relationships against annual ACD and annual mean temperature, annual precipitation and governance factors will be examined. The annual variations of forest C density might be subtle and difficult to separate but the changes will be prominent at a decadal scale as suggested (Myneni et al. 2001; Tan et al. 2007). The decadal ACD images of difference periods can be computed using raster calculator in spatial analyst tool of ArcGIS (Fig. 2). Because the estimated regional C density varied from 20 Mg C ha⁻¹ in dispersal and managed vegetative areas to > 40 Mg C ha⁻¹ in intact forested cover according to previous results (Fang

and Chen 2001; Tan et al. 2007; Zhang et al. 2013). Therefore, for expediency of comparisons, the ACD was divided into six categories, C1 (< 20 Mg C ha⁻¹), C2 (20–40 Mg C ha⁻¹), C3 (40–60 Mg C ha⁻¹), C4 (60–80 Mg C ha⁻¹), C5 (80–100 Mg C ha⁻¹), and C6 (> 100 Mg C ha⁻¹), respectively, to show the spatiotemporal patterns of C density in *Pinus massoniana* forest over time. The landscape structure and composition of six ACD categories of various periods were further analyzed using landscape metrics, please see the detail description in the section “The computation of landscape metrics.”

Ecological governance factors

In order to test the effects of ecological management on ACD dynamic, there were thirteen relative governance factors selected for correlation analysis, including forest replantation (ha); forest prohibited region (ha); grass plantation (ha); reconstruction of low-function forest (ha); economic forest plantation (ha); the mitigation of slope terrace (ha); governance of slid-valley (number); water-saving canal engineering (m); road construction (m); the subsidy of coal use fee (household; numbers); the subsidy of electricity use fee (household; numbers); the construction of biogas digester pool (household; numbers) and the household income (RMB). There were 4 years (2000, 2006, 2010, and 2015) of data that could be acquired from the water and Soil Conservation Bureau of Changting county (<http://www.changting.gov.cn/>).

The computation of landscape metrics

The spatiotemporal patterns of landscape dynamics can provide significant information about the disturbance history. Landscape metrics have been used as important indicators for monitoring regional environmental quality, and quantifications of ecological processes (Tischendorf 2001; Lausch and Herzog 2002; Bender et al. 2003). Studies suggested that the number of patches, patch size, edge and composition are critical for maintaining the function and integrity of forest ecosystems (Millington et al. 2003). Therefore, the metrics such as patch density (PD), mean patch size (MPS), interspersion and juxtaposition (IJI), and aggregation index (AI) are helpful for comprehending the interactions between ecosystem and landscape (Table 2). To quantify the spatial pattern of C storage of *Pinus massoniana* forest with the evolution of landscape over 35 years. We first converted the maps of *Pinus massoniana* distribution into grid format with 3 m resolution for each period under ARCGIS 10.3. Then, the grid maps were provided as input in FRAGSTATS, a spatial pattern analysis software (ver.4.2) developed by McGarigal (2014), to calculate the indices of six ACD categories for different time (Fig. 2).

Statistical analysis

The trends of C density and C storage over the 35 years and the relationships between C density and storage and climatic factors (temperature and precipitation) were analyzed using linear regression model. The correlation analysis was applied in the relationships between ACD of *Pinus massoniana* forest and the main ecological governance factors, and the statistical significance was set at p value < 0.05 . All statistical analyses were conducted in SPSS Statistics v.20.

Results

The spatial patterns of ACD on the topography

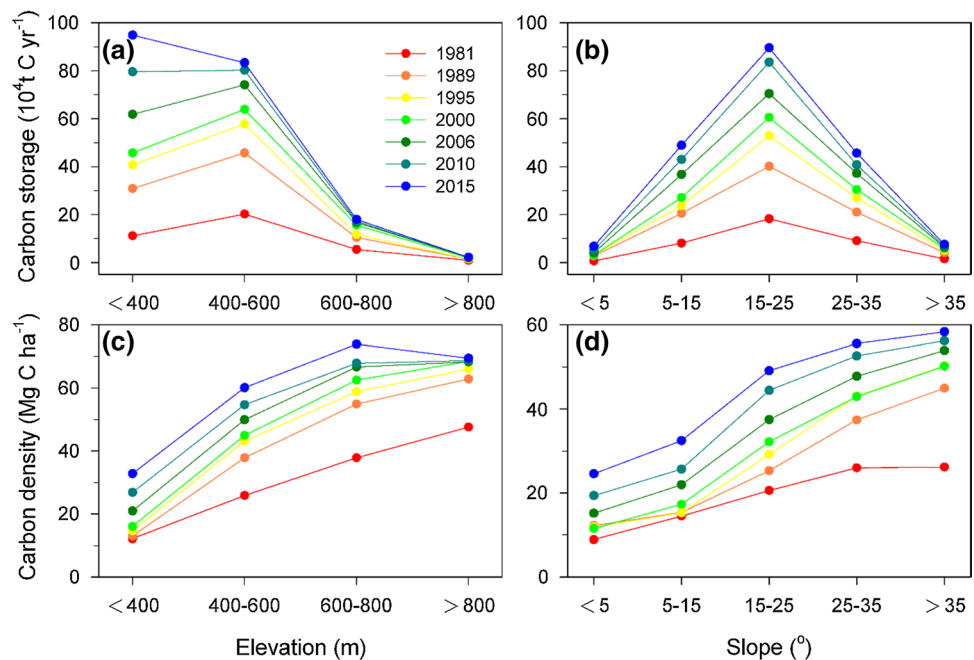
In 1981, the ACD of *Pinus massoniana* forest of all categories were scattered with only a few higher values in mountain areas surrounded by Hetian basin (Fig. 4). The ACD increased significantly over study regions for most categories from hillsides to mountain regions during 1981–2015, except for middle of basin ($p < 0.05$; Fig. 4).

The C storage showed increasing trends with elevational and slope gradients over time, for example the C storages increased from 11.12×10^4 t C in 1981 to 94.88×10^4 t C in 2015 at elevation < 400 m and increased from 0.93×10^4 t C in 1981 to 2.18×10^4 t C in 2015 at elevation > 800 m and same as other three elevational categories ($p < 0.05$; Fig. 5a). The patterns of C density revealed the similar upward trends with elevational gradient increasing from 12.16 Mg C ha⁻¹ in 1981 to 32.81 Mg C ha⁻¹ in 2015 at elevation < 400 m and increased from 47.59 Mg C ha⁻¹ in 1981 to 69.46 Mg C ha⁻¹ in 2015 at elevation > 800 m ($p < 0.05$; Fig. 5c). For slope gradient, the values of C storage were lower than 7.6×10^4 t C at lowest slope ($< 5^\circ$) and highest slope topography ($> 35^\circ$), but the highest C storages all appeared at slope 15 – 25° that increased from 18.26 Mg C ha⁻¹ in 1981 to 89.54 Mg C ha⁻¹ in 2015 ($p < 0.05$; Fig. 5b). The values of C density increased from 8.91, 14.84, 20.58, 25.97, and 26.16 Mg C ha⁻¹ in 1981 to 24.57, 32.84, 49.14 Mg C ha⁻¹, 55.57, and 58.34 Mg C ha⁻¹ in 2015 at slope categories $< 5^\circ$, 5 – 15° , 15 – 25° , 25 – 35° and $> 35^\circ$, respectively ($p < 0.05$; Fig. 5d).

Table 2 Definitions of landscape metrics

Name of landscape metrics	Explanations
Patch density (PD)	The number of patches of per 100 ha
Mean patch size (MPS)	The area occupied by a particular patch type divided by the number of patches of that type
Interspersion and Juxtaposition index (IJI)	The adjacency of each patch with all other forest types
Aggregation index (AI)	Class specific and independent of landscape composition

Fig. 5 The spatial variations of the carbon storage (10^4 t C yr^{-1}) and carbon density (Mg C ha^{-1}) of *Pinus massoniana* forest along elevational (a, c) and slope gradients (b, d). The increases in carbon storage and carbon density are all statistically significant ($p < 0.05$) at different elevational and slope gradients over 35 years



Based on the decadal scale with concurrent environmental policy, the frequency distribution revealed that 79% (1981–1989), 65% (1989–2000), and 93% (2000–2015) of forested regions for three periods showing an increasing trend in C density (Fig. 6). There were 20% and 10% of forested regions during first project and second project experienced decreases of C density (Fig. 6a, c); however, during intermission period about 35% forested region underwent a decrease (Fig. 6b). During the first period (1981–1989), the major distributions of positive C density trends were around the mountain while the negative C density concentrated on central and northern part of Changting county. During the intermission period (1989–2000), the positive C density distributed at central and northern, and the negative C density distributed widespread at the lower slope of study region (Fig. 6). In contrast, during the second project (after 2000), the C density revealed an overall upward trend across the region (Fig. 6).

Temporal dynamics of ACD over past three decades

The coverage of *Pinus massoniana* forest area increased from 18,710 ha in 1981 to 37,100 ha in 1989 with two folds, and then the coverage extended to 45,400 ha in 2000 with an increasing rate of 7600 ha per decade ($p < 0.05$; Fig. 7). The C storage in *Pinus massoniana* forest increased from 0.38 Tg C in 1981 to 1.98 Tg C in 2015, and the C density increased from 20.14 Mg C ha^{-1} in 1981 to 43.57 Mg C ha^{-1} in 2015, with an average annual growth rate of 4.7×10^3 Mg in C storage and 0.69 Mg C ha^{-1} in C density, respectively ($p < 0.05$; Fig. 7). The results were comparable to other estimations

of forest vegetation C density in China, 40–50 Mg C ha^{-1} (Fang and Chen 2001; Tan et al. 2007). There were significant positive relationships between annual mean temperature and C density and C storage ($r = 0.77$, $p < 0.05$), but no significant relationships were found between annual precipitation and C density or C storage ($r = 0.30$, $p = 0.50$).

The area of C1 increased from 11,840 ha in 1981 to 26,500 ha in 2000 then decreased to 15,300 in 2015 (Fig. 8a). The C2 showed the similar trend to C1 increasing from 4450 ha in 1981 to 8300 ha in 2006 then declined to 6870 ha in 2015 (Fig. 8b). But the relative coverage (%) of both C1 and C2 decreased from 61% and 23% in 1981 to 32% and 14% in 2015. In contrast, the coverages of C3, C4, C5, and C6 categories all increased significantly from 2163, 725, 141, and 31 ha in 1981 to 8350, 6570, 5400, and 5665 ha in 2015 ($p < 0.05$; Fig. 8c–f), and their relative coverage all increased from 0.2–11 to 11–17% over 35 years (Fig. 8c–f).

Landscape structure dynamics of ACD

The mean patch size (MPS) of C1 significant decreased from 7.9 ha in 1981 to 2.5 ha in 2015 ($p < 0.05$), C5 and C6 significant increased from 2.0 and 2.9 ha in 1981 to 3.8 and 4.7 ha, respectively ($p < 0.05$; Fig. 9a), while C2, C3, and C4 were stable around between 1.5 and 2.5 ha over time (Fig. 9a). The aggregation index (AI) of C1 and C2 decreased from 81% and 46% in 1981 to 73% and 35% in 2015, respectively ($p < 0.05$; Fig. 9b). The AI of C3, C4 and C5 presented some inter-annual variations but all stayed below 40% and AI of C6 showed clear increasing from 33% in 1981 to 67% in

Fig. 6 The spatial and frequency distribution of differences in rate of carbon density of *Pinus massoniana* forest in the study area between **a** 1981 and 1989 (first project), **b** 1989 and 2000 (intermission), and **c** 2000 and 2015 (second project)

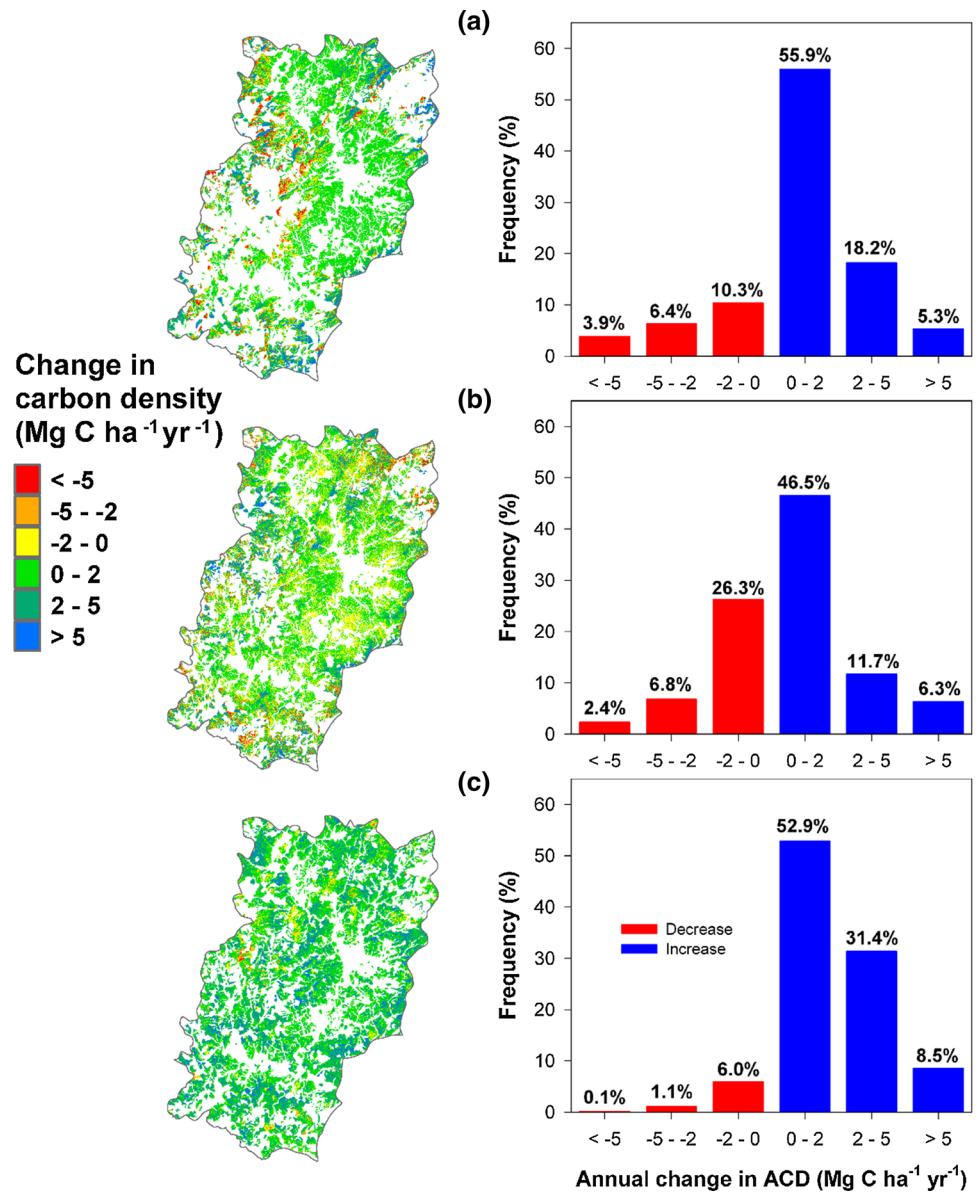


Fig. 7 The temporal trends of coverage, carbon storage and density of *Pinus massoniana* forest during 1981 and 2015. The increases in coverage of *Pinus massoniana* forest area, carbon storage and carbon density of entire study region are all statistically significant ($p < 0.05$) over 35 years

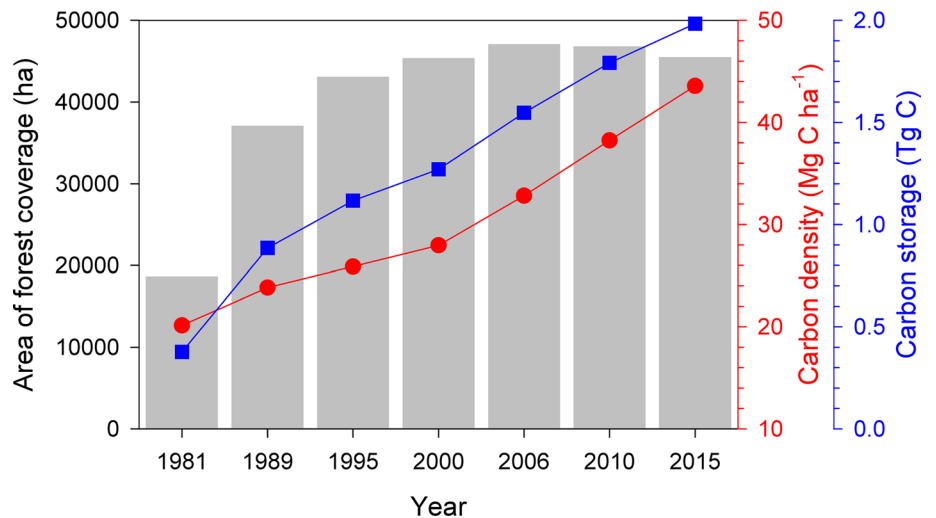


Fig. 8 The temporal patterns of six various categories (C1–C6) of carbon density of *Pinus massoniana* forest in the study area. The C1, C2, C3, C4, C5, and C6 categories of ACD levels stand for <20, 20–40, 40–60, 60–80, 80–100, >100 Mg C ha⁻¹, respectively. The increases of carbon density in C3, C4, C5, and C6 of entire study region are statistically significant ($p < 0.05$) over 35 years, but not for C1 and C2

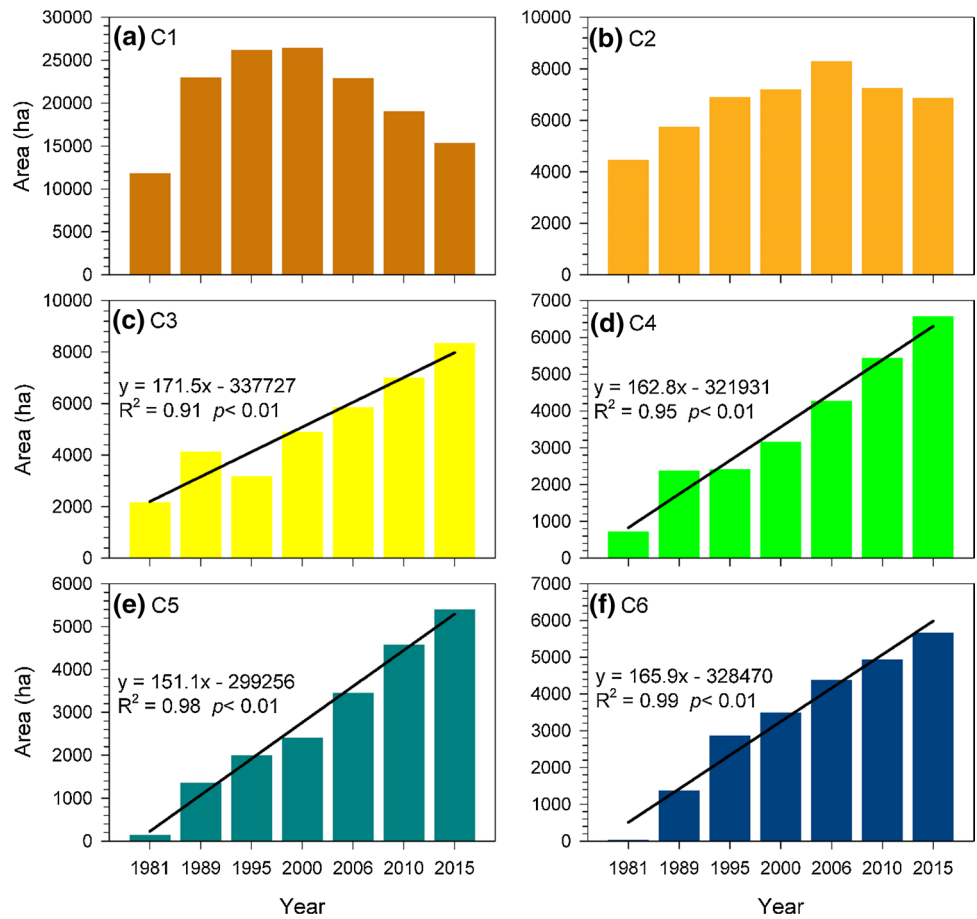
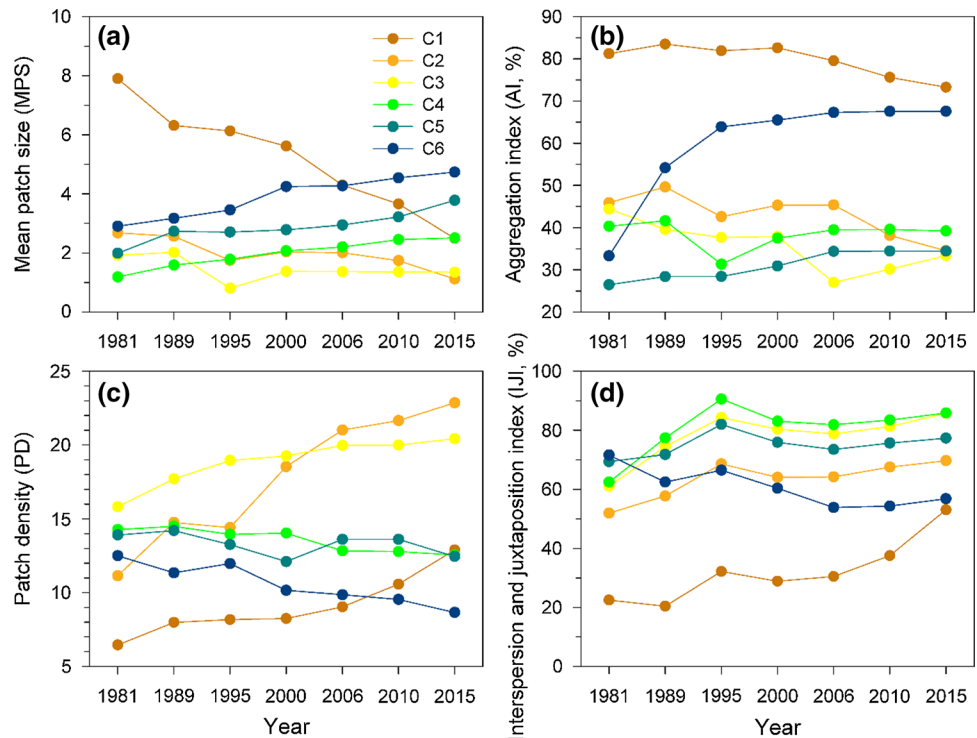


Fig. 9 Landscape metrics of six categories of carbon density for *Pinus massoniana* forest in the study area from 1981 to 2015. **a** Mean patch size (MPS), **b** aggregation index (AI), **c** patch density (PD), and **d** interspersions and juxtaposition index (IJI)



2015 ($p < 0.05$; Fig. 9b). The patch density (PD) of C1, C2, and C3 showed upward trends from 6.5, 11.1, and 15.8 in 1981 to 12.9, 22.9, and 20.4 in 2015, respectively ($p < 0.05$). In contrast, the PD of C4, C5 and C6 exhibited somewhat decreases from 14.3, 13.9, and 12.5 in 1981 to 12.5, 12.5 and 8.7 in 2015 ($p < 0.05$; Fig. 9c). The interspersion and juxtaposition index (IJI) of the C1, C2, C3, C4 and C5 grade appears rising trend, except C6 of a downward trend ($p < 0.05$; Fig. 9d).

Forest recovery in human dominated area

Although the C density was always lowest surrounded by residential areas for different periods (< 200 m in distance from village; Fig. 10a), the C density of *Pinus massoniana* forest showed a significant increase from regions nearby village to distance far from village 1500 m, for example the C density increased from 12.4 Mg C ha⁻¹ in 1981 to 28.8 Mg C ha⁻¹ in 2015 at 50 m and increased from 21.0 Mg C ha⁻¹ in 1981 to 39.3 Mg C ha⁻¹ in 2015 at 1500 m ($p < 0.05$; Fig. 10a). The C density near village had slower recovery

(16 Mg C ha⁻¹) from 1981 to 2015 than the distance 1500 m away (20 Mg C ha⁻¹) ($p < 0.05$; Fig. 10a).

The C density during two periods with ecological management (first project during 1981–1989 and second project during 2000–2015) showed a higher increasing rate (25–48%) than the intermission period (9–18%) during 1989–2000 ($p < 0.05$; Fig. 10b). The higher increasing rate of C density during two projects occurred within 400 m to residential regions (Fig. 10b).

The influences of governance factors on ACD

The correlation analysis showed that the seven of the governance and management factors significant affected that ACD changes, including the forest replantation ($r = 0.993$, $p < 0.01$), forest prohibited region ($r = 0.990$, $p < 0.05$), grass plantation ($r = 0.963$, $p < 0.05$), governance of slid-valley ($r = 0.999$, $p < 0.01$), road construction ($r = 0.976$, $p < 0.05$), electricity subsidies ($r = 0.959$, $p < 0.05$), and income ($r = 0.970$, $p < 0.05$) (Table 3).

Discussion

The significant increases in coverage, C density and storage of *Pinus massoniana* forest in Changting county over the past 35 years were attributed to the prohibitions against human activities, and the utilization of ecological engineering to stabilize vulnerable landscape erosion under the eco-compensation projects. The average vegetation coverage of Hetian basin increased from 30.83% in 1981 to 39.3% in 1989 during the first project (Xu et al. 2016b),

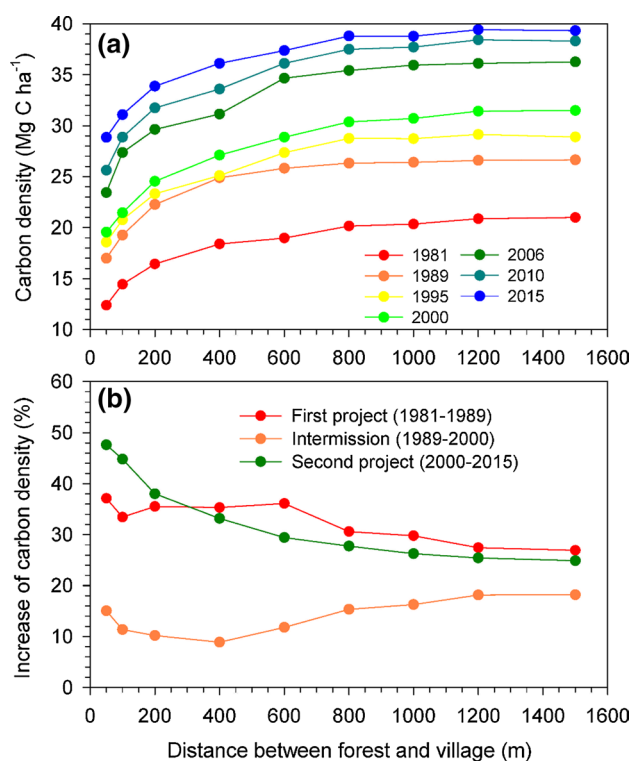


Fig. 10 The patterns of carbon density of *Pinus massoniana* (a), and the increased rate of carbon density among three different periods (please refer to the description in section Study area) with increasing distance from village (b). The increases of carbon density from regions nearby village to distance 1500 m far from village of entire study region are all statistically significant ($p < 0.05$) between 1981 and 2015

Table 3 The correlation coefficients between governance factors and ACD changes during 1981–2015

Governance factors	Correlation coefficients
Forest replantation (ha)	0.993**
Forest prohibited region (ha)	0.990*
Grass plantation (ha)	0.963*
Reconstruction of low-function forest (ha)	0.943
Economic forest plantation (ha)	0.943
The mitigation of slope terrace (ha)	0.913
Governance of slid-valley (numbers)	0.999**
Water-saving canal engineering (m)	0.931
Road construction (m)	0.976*
The subsidy of coal use fee (household; numbers)	0.821
The subsidy of electricity use fee (household; numbers)	0.959*
The construction of biogas digester pool (numbers)	0.862
Income (RMB)	0.970*

p -value: ** < 0.01 ; * < 0.05

and consequent the sediment yields decreased from 5000 to 12,000 t km⁻² in 1981 to 449–695 t km⁻² in 1989 (Yang et al. 2005a). In the second project, the vegetation coverage further increased from 46.53% in 2000 to 60.34% in 2013 (Xu et al. 2016b). Wang et al. (2016) suggested that the closing hillsides and mountains for forest recovery was the most cost-effective management, following by the forest fertilizing and planting trees and grass, which confirmed with the results in the study (Table 3). This indicates that the practice of ecological management for forested regions is helpful to control soil loss and improve the forest productivity. Furthermore, the young stage of forest ecosystem (< 40 year-old) in this region implies that there is a great potential for C sequestration in near future (Vayreda et al. 2012; Yan et al. 2015).

Studies suggested that the policy considering local economic development, family income, and social factors such as eco-compensation and road construction, were also crucial for ACD increase in *Pinus massoniana* forest (Mu et al. 2013; Xu et al. 2016a). In the study, the significant correlations between ACD and governance factors such as forest and grass plantation and management of slid-valley indicated that the reforestation and plantation and mitigation of erosive of gullies and valleys directly stabilize the degraded landscape (Table 3). The road construction might be related to eco-tourism which increased the employment for local people and indirectly reduced the requirements depended on land exploitation (Fan et al. 2018). The subsidy for coal and electricity utilization instead of timber harvest for firewood also improved the usage of energy and promoted the recovery of vegetation growth and forest C reserve. Cao et al. (2009) indicated that paying residents to established pig farms, fish ponds and planting fruits trees helped to build up a reliable long-term industry supporting the livelihood of local people without impairing the environment. A recent study also revealed that the annual growth of C storage (3.52%) of *Pinus massoniana* forest within the managed region in Changting county was higher than regions outside of Changting county without management (1.76%) during 2000 and 2013 (Xu et al. 2016a).

In addition to the ecological management policy, the increasing emigration from rural to urban regions due to the disparities of economic development also help decreasing human interventions over the past two decades (Xu et al. 2016b). The strategy of long-term support from governmental authority to meet the basic living of local farmer and people is necessary for approaching a stable and health ecosystem (Mez-Pompa and Kaus 1999). For example, the Fujian province provided the subsidies for restricting timber harvest and the farmers were get paid (30 RMB per day) and were encouraged to plant trees (Cao et al. 2009). This is evident that two project periods (1981–1989 and 2000–2015) showed higher increasing rate of C density

compared to intermission period (1989–2000) (Fig. 10b). To overcome the dilemma of regional economy and ecological degradation, it will be necessary to keep into consideration of green agriculture and to innovate the structure of industrial production (Fraser et al. 2003). The enforcement of authority and the ban on illegal timber harvest and mining in ecological protection regions have been suggested to ameliorate ecosystem restoration and succession, and then the following biodiversity issue should be also put in a high priority (Haque et al. 2014; Arasa-Gisbert et al. 2018). The re-investigation is necessary to the densely inhabited regions with applications of ecological governance policy in the future. The long-term sustainable environment depends on how the policy makers could efficiently get rid of poverty of residents in the region over time that will truly better both the environment and community.

The C density of *Pinus massoniana* forest increased with the increasing elevation and slope (Fig. 5), indicating that there was a great potential for forest C sequestration and accumulation in the region with less anthropogenic disturbances and vice versa. The productivity of a young *Pinus massoniana* forest (5-year-old) in a national conserved region in northwest Fujian showed that the productivity of at downslope and flat region was higher than that at upslope (Huang 2002). In contrast, in this study the spatiotemporal patterns of various categories of C density of *Pinus massoniana* forest improved significantly with similar increment over the entire landscape regardless of elevational and slope gradients over the past three decades, in which the higher elevational and slope categories usually had higher C density (Fig. 5c, d). From the landscape structure of C density over time, the increasing of larger mean patch size (MPS) in higher C density patches (C4–C6) but decreasing in lower C density patches (C1–C3) indicated that the degree of fragmentation lowered over time (Gautam et al. 2003). The reverse patterns of patch density (PD) on higher and lower C density patches also proved this trend. The aggregation index (AI) of C1–C5 showed some decreases but C6 boosted manifest from 33 to 70% over 35 years ($p < 0.05$) demonstrating that the spatial connectivity bettered (Li et al. 2012). The some increasing (decreasing) of lower (higher) C density of Interspersion and Juxtaposition index (IJI) also suggested that the landscape gradually shifted from lower C density to higher C density conditions. The differences of C density improvement between project-support and intermission periods showed that the contribution of policy governance was helpful (Fig. 10b). The higher enhancement of C density nearby the village (within 400 m) during two project-support periods compared to intermission period demonstrated that proscribed management was effective to forest recovery.

Shono et al. (2007) indicated that natural regeneration in many degraded forestlands is low and slow subjected to intensive anthropogenic disturbance and consequent

the nutrient depletion and isolation from intact forests. In a manipulation experiment in watershed scale at central Fujian, Yang et al. (2018) showed that assisted natural regeneration (ANR) of native *C. carlesii* forest reduced surface runoff and sediment yield up to 50% compared with other young plantations in the first 3 years and above-ground biomass of the young ANR forest was also approximately 3–4 times of that of other young plantations. The ANR in the region is suggested as a simple and effective treatment to convert degraded lands into more productive forests with plenty of C storage by minimizing barriers to natural regeneration such as soil degradation and competition with weedy species (Ganz and Durst 2003; Shoo and Catterall 2013). A study combined in situ observations and remote sensing in the USA indicated that reforesting lands (> 500,000 km²) will gain 13–21 Tg of topsoil C storage annually, which also offset 1% at least of US greenhouse gas emissions (Nave et al. 2018). Therefore, maximizing the C storage of *Pinus massoniana* reforestation with in degraded environment in southeastern China will not only improve soil stability but also help to sequester elevating atmospheric C.

Although the estimations of aboveground C density and C storage varied regions by regions due to their differences of forest ecosystem and environmental conditions, the outcome in our study was comparable to previous works (Fang and Chen 2001; Tan et al. 2007). It indicated that the approach used in the analysis was feasible and acceptable. Yet there are still some limitations at the current evaluations without more considerations, such as soil factors belowground and the varieties of climate over the past three decades. Recent studies showed that the soil organic C (SOC) content of the forest plots decreased slightly with the recovery time of *Pinus massoniana* forest (He et al. 2013; Xie et al. 2013; Jiang et al. 2018). It needs further examinations to ascertain the contributions of belowground C dynamics to above-ground C storage. Furthermore, studies showed that the warming climate have significantly impacted the vegetation growth and productivity in global scale (Wang et al. 2011b; Gottfried et al. 2012; Kim et al. 2014), and it seems that the significant positive relationship between concurrent ACD and annual mean temperature showing the same finding. Nevertheless, a recent study exhibited that the vegetation coverage in Hetian basin increased from 49% in 1988 to 60% in 2010 which resulted in lowering the regional land surface temperature by 0.6–1.0 °C (Xu et al. 2013), the discrepancy might derive from the different time resolution of data used. It also complicates the interactions between climate and vegetation productivity and C sequestration in regions. Because the heavy anthropogenic interventions might surpass the climatic factors on the dynamics of vegetation growth and C budget in study area over the last decades in Changting county. The effects of warming scenarios will need further

examinations following recovery of forest ecosystem with if less management in the future.

Conclusions

The spatiotemporal patterns of forest C density and C storage were estimated in a soil-degraded region in Changting county, southeast China, between 1981 and 2015 based on the combination of in situ survey and remotely sensed images. The C density in *Pinus massoniana* forest increased from 20.14 Mg C ha⁻¹ in 1981 to 43.57 Mg C ha⁻¹ in 2015, and the C storage in the study region increased from 0.38 Tg C in 1981 to 1.98 Tg C in 2015. The significant increasing C sequestration indicated that the ecological management and eco-compensation policy implemented in this region is powerful for mitigation of soil erosion, recovery of afforestation and consequent C storage. There is a large potential of C accumulation due to the recovery of susceptible forest ecosystems, like Changting county, and will contribute to alleviate the elevating global atmospheric C emission.

Acknowledgements We are grateful to the Soil and Water Conservation, the Statistics Bureau, and the Forestry Bureau of Changting county for providing valuable data and the assistances in the field work. We also thank Prof. T.C. Lin of National Taiwan Normal University for his valuable comments on this manuscript. This study was supported by grants from the National Key R&D Program of China (Grant No. 2017YFD0600903), National Natural Science Foundation of China (Grant No. 41771370) and High-resolution Earth Observation Project of China (Grant No. 03-Y20A04-9001-17/18, 30-Y20A07-9003-17/18). CT Chang acknowledges the support from the Ministry of Science and Technology, Taiwan (MOST 105-2410-H-029-056-MY3).

Compliance with ethical standards

Conflict of interest The authors declare that they have no conflict of interest.

References

- Arasa-Gisbert R, Vayreda J, Román-Cuesta RM, Vilella SA, Mayorga R, Retana J (2018) Forest diversity plays a key role in determining the stand carbon stocks of Mexican forests. *For Ecol Manag* 415–416:160–171. <https://doi.org/10.1016/j.foreco.2018.02.023>
- Asner GP, Clark JK, Mascaro J, Vaudry R, Chadwick KD, Vieilledent G et al (2012) Human and environmental controls over above-ground carbon storage in Madagascar. *Carbon Balance Manag* 7(2):1–13. <https://doi.org/10.1186/1750-0680-7-2>
- Bender DJ, Tischendorf L, Fahrig L (2003) Using patch isolation metrics to predict animal movement in binary landscapes. *Landsc Ecol* 18:17–39. <https://doi.org/10.1023/A:1022937226820>
- Canadell JG, Raupach MR (2008) Managing forest for climate change mitigation. *Science* 320:1456–1457. <https://doi.org/10.1126/science.1155458>
- Cao SX, Zhong BL, Yue H, Zeng HS, Zeng JH (2009) Development and testing of a sustainable environmental restoration policy on eradicating the poverty trap in China's Changting County.

- Proc Natl Acad Sci USA 106(26):10712–10716. <https://doi.org/10.1073/pnas.0900197106>
- Cheng R, Feng X, Xiao W, Wang R, Wang X, Du H (2011) Response of net productivity of masson pine plantation to climate change in North subtropical region. *Acta Ecol Sin* 31(8):2086–2095 (in Chinese)
- Das A, Ghosh PK, Lal R, Saha R, Ngachan S (2017) Soil quality effects on conservation practices in maize-rapeseed system in eastern Himalaya. *Land Degrad Dev* 28:1862–1874. <https://doi.org/10.1002/ldr.2325>
- Dixon RK, Brown S, Houghton RA, Solomon AM, Trexler MC, Wisniewski J (1994) Carbon pools and flux of global forest ecosystem. *Science* 263:185–190. <https://doi.org/10.1126/science.263.5144.185>
- Dong J, Kaufmann RK, Myneni RB, Tucker CJ, Kauppi PE, Liski J, Buermann W, Hughes MK (2003) Remote sensing estimates of boreal and temperate forest woody biomass: carbon pools, sources, and sinks. *Remote Sens Environ* 84:393–410. [https://doi.org/10.1016/S0034-4257\(02\)00130-X](https://doi.org/10.1016/S0034-4257(02)00130-X)
- Dubayah RO, Sheldon SL, Clark DB, Hofton MA, Blair JB, Hurtt GC, Chazdon RL (2015) Estimation of tropical forest height and biomass dynamics using lidar remote sensing at La Selva, Costa Rica. *J Geophys Res* 115(G2):272–281. <https://doi.org/10.1029/2009JG000933>
- Fan SL, Zhang SS, Qiu LJ, Wang PJ, Huang YH (2018) Coordination relationship between ecological environment construction and economic development in Changting County, Fujian Province. *J China Agric Univ* 23(3):175–184. <https://doi.org/10.11841/j.issn.1007-4333.2018.03.21> (in Chinese)
- Fang JY (2000) Forest biomass carbon pool of middle and high latitudes in the north hemisphere is probably much smaller than present estimates. *Chin J Plant Ecol* 24(5):635–638. <https://doi.org/10.3321/j.issn:1005-264X.2000.05.022> (in Chinese)
- Fang JY, Chen AP (2001) Dynamic forest biomass carbon pools in China and their significance. *Acta Bot Sin* 43(9):967–973. <https://doi.org/10.3321/j.issn:1672-9072.2001.09.014> (in Chinese)
- Feng X, Cheng R, Xiao W, Wang R, Wang X, Gao B (2011) Effects of air temperature in growing season on Masson pine (*Pinus massoniana*) radial growth in north subtropical region of China. *Chin J Ecol* 30(4):650–655 (in Chinese)
- Fraser EDG, Mabee W, Slaymaker O (2003) Mutual vulnerability, mutual dependence: the reflexive relation between human society and the environment. *Glob Environ Chang* 13:137–144. [https://doi.org/10.1016/S0959-3780\(03\)00022-0](https://doi.org/10.1016/S0959-3780(03)00022-0)
- Ganz DJ, Durst PB (2003) Assisted natural regeneration: an overview. In: Dugan PC, et al. (Eds), *Advancing assisted natural regeneration (ANR) in Asia and the Pacific*. RAP Publication, Bangkok, pp 1–4. Retrieved from <http://www.fao.org/docrep/004/ad466e/ad466e03.htm>
- Gao CB, Liu YQ (1992) Water and soil conservation stand of black wattle and its ecological- economic benefit analysis. *For Res* 5(1):32–38 (in Chinese)
- Gautam AP, Webb EL, Shivakoti GP, Zoebisch MA (2003) Land use dynamics and landscape change pattern in a mountain watershed in Nepal. *Agric Ecosyst Environ* 99(1–3):83–96. [https://doi.org/10.1016/S0167-8809\(03\)00148-8](https://doi.org/10.1016/S0167-8809(03)00148-8)
- Goetz S, Dubayah R (2011) Advances in remote sensing technology and implications for measuring and monitoring forest carbon stocks and change. *Carbon Manag* 2:231–244. <https://doi.org/10.4155/cmt.11.18>
- Gottfried M, Pauli H, Futschik A, Akhalkatsi M, Barančok P, Alonso JLB et al (2012) Continent-wide response of mountain vegetation to climate change. *Nat Clim Chang* 2(2):111–115. <https://doi.org/10.1038/nclimate1329>
- Han LL, Xie JS, Zeng HD, Xu C, He SJ, Yang YS (2013) Effects of *Paspalum notatum* flügge on carbon storage change and allocation in an ecosystem developed on degraded red Soil. *J Subtrop Res Environ* 8(1):33–40. <https://doi.org/10.3969/j.issn.1673-7105.2013.01.007> (in Chinese)
- Hao FH, Chang Y, Ning D (2004) Assessment of China's economic loss resulting from the degradation of agricultural and in the end of 20th century. *J Environ Sci* 16:199–203. <https://doi.org/10.3321/j.issn:1001-0742.2004.02.006>
- Haque N, Hughes A, Seng L, Vernon C (2014) Rare earth elements: overview of mining, mineralogy, uses, sustainability and environmental impact. *Resources* 3(4):614–635. <https://doi.org/10.3390/resources3040614>
- He SJ, Xie JS, Zeng HD, Tian H, Zhou YX, Xu C, Lyu MK, Yang YS (2013) Dynamic of soil organic carbon pool after restoration of *Pinus massoniana* in eroded red soil area. *Acta Ecol Sin* 33(10):2964–2973. <https://doi.org/10.5846/stxb201205180742> (in Chinese)
- Homer C, Huang CQ, Yang LM, Wylie B, Coan M (2003) Development of a 2001 national landcover database for the United States [EB/OL]. http://landcover.usgs.gov/Pdf/nlcd_pub_august.pdf
- Hou XL, Bai GS, Cao QY (1996) Study on benefits of soil and water conservation of forest and its mechanism in loess hilly region. *Res Soil Water Conserv* 3(2):98–103 (in Chinese)
- Houghton RA (2003) Why are estimates of the terrestrial carbon balance so different? *Global Chang Biol* 9(4):500–509. <https://doi.org/10.1046/j.1365-2486.2003.00620.x>
- Houghton RA, Butman D, Bunn AG, Krankina ON, Schlesinger P, Stone TA (2007) Mapping Russian forest biomass with data from satellites and forest inventories. *Environ Res Lett* 2(4):45032. <https://doi.org/10.1088/1748-9326/2/4/045032>
- Huang C (2002) The productivity of 5-year-old young *Pinus massoniana* forest on different site conditions and its distribution. *J Fujian For Sci Technol* 29(4):17–20. <https://doi.org/10.13428/j.cnki.fjlk.2002.04.006> (in Chinese)
- Huang SL, Xu HQ, Zeng HD, Liu ZC, Lin W (2013) Analysis of spatial and temporal dynamics of carbon storage of *Pinus massoniana* forest in the Hetian basin in County Changting of Fujian Province, China. *Earth Sci* 38(5):1081–1090. <https://doi.org/10.3799/dqkx.2013.106> (in Chinese)
- Jain AK, Yang X (2005) Modeling the effects of two different land cover change data sets on the carbon stocks of plants and soils in concert with CO₂ and climate change. *Glob Biogeochem Cycles* 19:GB2015. <https://doi.org/10.1029/2004GB002349>
- Jiang MH, Lyu MK, Lin WS, Xie JS, Yang YS (2018) Effects of ecological restoration on soil organic carbon components and stability in a red soil erosion area. *Acta Ecol Sin* 38(13):4861–4868. <https://doi.org/10.5846/stxb201707271358> (in Chinese)
- Kim Y, Kimball JS, Didan K, Henebry GM (2014) Response of vegetation growth and productivity to spring climate indicators in the conterminous United States derived from satellite remote sensing data fusion. *Agr For Meteorol* 194(194):132–143. <https://doi.org/10.1016/j.agrformet.2014.04.001>
- Lausch A, Herzog F (2002) Applicability of landscape metrics for the monitoring of landscape change: issues of scale, resolution and interpretability. *Ecol Indic* 2:3–15. [https://doi.org/10.1016/S1470-160X\(02\)00053-5](https://doi.org/10.1016/S1470-160X(02)00053-5)
- Li YY, Shao MA (2006) Changes of soil physical properties under long-term natural vegetation restoration in the Loess Plateau of China. *J Arid Environ* 64:77–96. <https://doi.org/10.1016/j.jaridenv.2005.04.005>
- Li XF, Chen ZB, Chen CM, Chen ZQ (2012) The study of landscape pattern of Fuzhou Gushan scenic spot. *J Fujian Norm Univ* 28(5):95–100. <https://doi.org/10.3969/j.issn.1000-5277.2012.05.019> (in Chinese)
- Liu J, Li S, Ouyang Z, Tam C, Chen X (2008) Ecological and socioeconomic effects of China's policies for ecosystem

- services. *Proc Natl Acad Sci USA* 105:9477–9482. <https://doi.org/10.1073/pnas.0706436105>
- Liu YC, Wang QF, Yu GR, Zhu XJ, Zhan XY, Guo Q, Yang H, Li SG, Hu ZM (2011) Ecosystems carbon storage and carbon sequestration potential of two main tree species for the Grain for Green Project on China's hilly Loess Plateau. *Acta Ecol Sin* 31(15):4277–4286 (in Chinese)
- Louks CJ, Lü Z, Dinerstein E, Wang H, Olson DM, Zhu C, Wang D (2001) Giant Pandas in a changing landscape. *Science* 294(5546):1465. <https://doi.org/10.1126/science.1064710>
- Luo X (1994) Discussion on the plant community succession in Hetian erosion area. *Bull Soil Water Conserv* 14(3):48–51 (in Chinese)
- Madugundu R, Nizalapur V, Jha CS (2008) Estimation of LAI and above-ground biomass in deciduous forests: Western Ghats of Karnataka, India. *Int J Appl Earth Obs Geoinf* 10:211–219. <https://doi.org/10.1016/j.jag.2007.11.004>
- McGarigal K (2014) *Fragstat 4.2. help*. University of Massachusetts, Amherst. <http://www.umass.edu/landeco/research/fragstats/documnts/fragstats.help.4.2.pdf>
- Mekonnen M, Keesstra SD, Stoosnijder L, Baartman JE, Margoulis J (2014) Soil conservation through sediment trapping: a review. *Land Degrad Dev* 26:544–556. <https://doi.org/10.1002/ldr.2308>
- Mez-Pompa AG, Kaus A (1999) From pre-Hispanic to future conservation alternatives: lessons from Mexico. *Proc Natl Acad Sci USA* 96:5982–5986. <https://doi.org/10.1073/pnas.96.11.5982>
- Millington AC, Velez-liendo XM, Bradley AV (2003) Scale dependence in multitemporal mapping of forest fragmentation in Bolivia: implications for explaining temporal trends in landscape ecology and applications to biodiversity conservation. *ISPRS J Photogramm* 57(4):289–299. [https://doi.org/10.1016/S0924-2716\(02\)00154-5](https://doi.org/10.1016/S0924-2716(02)00154-5)
- Mu S, Zhou S, Chen Y, Li J, Ju W, Odeh IOA (2013) Assessing the impact of restoration-induced land conversion and management alternatives on net primary productivity in Inner Mongolian grassland, China. *Glob Planet Chang* 108:29–41. <https://doi.org/10.1016/j.gloplacha.2013.06.007>
- Myneni RB, Dong J, Tucker CJ, Kaufmann RK, Kauppi PE, Zhou L, Alexeyev V, Hughes MK (2001) A large carbon sink in the woody biomass of northern forests. *Proc Natl Acad Sci USA* 98:1484–1489. <https://doi.org/10.1073/pnas.261555198>
- Nave LE, Swanston CW, Curtis PS (2010) Harvest impacts on soil carbon storage in temperate forests. *For Ecol Manag* 259:857–866. <https://doi.org/10.1016/j.foreco.2009.12.009>
- Nave LE, Domke GM, Hofmeister KL, Mishra U, Perry CH, Walters BF, Swanston CW (2018) Reforestation can sequester two petagrams of carbon in US topsoils in a century. *Proc Natl Acad Sci USA* 115:2776–2781. <https://doi.org/10.1073/pnas.1719685115>
- Nemani R, Votava P, Michaelis A, Melton AM, Milesi C (2013) Collaborative supercomputing for global change science. *EOS* 92(13):109–110. <https://doi.org/10.1029/2011EO130001>
- Olson JS, Watts JA, Allison LJ (1983) Carbon in live vegetation of major world ecosystem. Technical Report. U. S. Washington: Department of Energy
- Pan YD, Birdsey RA, Fang JY, Houghton R, Kauppi PE, Kurz WA et al (2011) A large and persistent carbon sink in the world's forest. *Science* 333(6045):988–993. <https://doi.org/10.1126/science.1201609>
- Persha L, Agrawal A, Chhatre A (2011) Social and ecological synergy: local rulemaking, forest livelihoods and biodiversity conservation. *Science* 331:1606–1608. <https://doi.org/10.1126/science.1199343>
- Piao S, Fang J, Zu B, Tan K (2005) Forest biomass carbon stocks in China over the past 2 decades: estimation based on integrated inventory and satellite data. *J Geophys Res* 110:G01006. <https://doi.org/10.1029/2005JG000014>
- Piao S, Ciais P, Friedlingstein P, de Noblet-Ducoudré D, Cadule P, Viovy N, Wang T (2009) Spatiotemporal patterns of terrestrial carbon cycle during the 20th century. *Glob Biogeochem Cycles* 23:GB4026. <https://doi.org/10.1029/2008gb003339>
- Ramsey RD, Wright DLJ, McGinty C (2004) Evaluating the use of Landsat 30 m enhanced thematic mapper to monitor vegetation cover in shrub-steppe environments. *Geocarto Int* 19(2):39–47. <https://doi.org/10.1080/10106040408542305>
- Ren Y, Yan J, Wei X, Wang Y, Yang Y, Hua L, Xiong Y, Niu X, Song X (2012) Effects of rapid urban sprawl on urban forest carbon stocks: integrating remotely sensed, GIS and forest inventory data. *J Environ Manag* 113:447–455. <https://doi.org/10.1016/j.jenvman.2012.09.011>
- Saatchi SS, Harris NL, Brown S, Lefsky M, Mitchard ETA, Salas W (2011) Benchmark map of forest carbon stocks in tropical regions across three continents. *Proc Natl Acad Sci USA* 108:9899–9904. <https://doi.org/10.1073/pnas.1019576108>
- Sanchez-Azofeifi GA, Castro-Esau KL, Kurz WA, Joyce A (2009) Monitoring carbon stocks in the tropics and the remote sensing operational limitations: from local to regional projects. *Ecol Appl* 19:480–494. <https://doi.org/10.1890/08-1149.1>
- Sehott JR, Selvaggio C, Volchok WJ (1988) Radiometric scene normalization using pseudo-invariant features. *Remote Sens Environ* 26:1–16. [https://doi.org/10.1016/0034-4257\(88\)90116-2](https://doi.org/10.1016/0034-4257(88)90116-2)
- Shono K, Cadaweng EA, Durst PB (2007) Application of assisted natural regeneration to restore degraded tropical forestlands. *Restor Ecol* 15(4):620–626. <https://doi.org/10.1111/j.1526-100X.2007.00274.x>
- Shoo LP, Catterall CP (2013) Stimulating natural regeneration of tropical forest on degraded land: approaches, outcomes, and information gaps. *Restor Ecol* 21(6):670–677. <https://doi.org/10.1111/rec.12048>
- Sun H (2011) Soil erosion problems and preventing countermeasures in China. *China Water Resour* 6:16–21. <https://doi.org/10.3969/j.issn.1000-1123.2011.06.008>
- Tan K, Piao S, Peng C, Fang J (2007) Satellite-based estimation of biomass carbon stocks for northeast China's forests between 1982 and 1999. *For Ecol Manag* 240:114–121. <https://doi.org/10.1016/j.foreco.2006.12.018>
- Tischendorf L (2001) Can landscape indices predict ecological processes consistently? *Landsc Ecol* 16:235–254. <https://doi.org/10.1023/A:1011112719782>
- Vayreda J, Gracia M, Canadell JG, Retana J (2012) Spatial patterns and predictors of forest carbon stocks in Western Mediterranean. *Ecosystems* 15:1258–1270. <https://doi.org/10.1007/s1002-012-9582-7>
- Wang C, Yang Y, Zhang Y (2011a) Economic development, rural livelihoods, and ecological restoration: evidence from China. *Ambio* 40:78–87. <https://doi.org/10.1007/s13280-010-0093-5>
- Wang X, Piao S, Ciais P, Li J, Friedlingstein P, Koven C et al (2011b) Spring temperature change and its implication in the change of vegetation growth in north America from 1982 to 2006. *Proc Natl Acad Sci USA* 108(4):1240–1245. <https://doi.org/10.1073/pnas.1014425108>
- Wang C, Yang Y, Zhang Y (2012) Rural household livelihood change, fuelwood substitution, and hilly ecosystem restoration: evidence from China. *Renew Sustain Energy Rev* 16(5):2475–2482. <https://doi.org/10.1016/j.rser.2012.01.070>
- Wang YF, Liu L, Li ZC, Shangguan ZP (2015) Carbon storage and carbon density of forest vegetation in Luoyang, Western Henan Province. *Acta Prataculturae Sin* 24(10):1–11. <https://doi.org/10.11686/cyxb2015078> (in Chinese)
- Wang C, Yang Y, Zhang Y (2016) Cost-effective targeting soil and water conservation: a case study of Changting County in southeast China. *Land Degrad Dev* 27:387–394. <https://doi.org/10.1002/ldr.2397>
- Wu GS, Wang HY (2011) Spatial and temporal analysis of soil erosion in typical areas: a case study of the Hetian Town of County

- Changting. *Straits Sci* 6:19–24. <https://doi.org/10.3969/j.issn.1673-8683.2011.06.006> (in Chinese)
- Xie JS, Yang YY, Xie MS (2004) Ecological restoration technology and degradation of eroded granite red soil in subtropical regions in China. *Res Soil Water Conserv* 11(3):154–156. <https://doi.org/10.3969/j.issn.1005-3409.2004.03.045> (in Chinese)
- Xie J, Guo J, Yang Z, Huang Z, Chen G, Yang Y (2013) Rapid accumulation of carbon on severely eroded red soils through afforestation in subtropical China. *For Ecol Manag* 300:53–59. <https://doi.org/10.1016/j.foreco.2012.06.038>
- Xu HQ (2008) Comparison of the models for the normalization of Landsat imagery. *J Geo-Infor Sci* 10(3):294–301. <https://doi.org/10.3969/j.issn.1560-8999.2008.03.004> (in Chinese)
- Xu HQ, He H, Huang SL (2013) Analysis of fractional vegetation cover change and its impact on thermal environment in the Hetian basic area of County Changting, Fujian Province, China. *Acta Ecol Sin* 33(10):2954–2963. <https://doi.org/10.5846/stxb201205150720> (in Chinese)
- Xu KJ, Xie JS, Zeng HD, Lü MK, Ren J, Yang YS (2016a) Driving factors and spatiotemporal dynamics of carbon storage of a *Pinus massoniana* plantation in reddish soil erosion region with ecological restoration. *Sci Soil Water Conserv* 14(1):89–96. <https://doi.org/10.16843/j.sswc.2016.01.011> (in Chinese)
- Xu KJ, Zeng HD, Ren J, Xie JS, Yang YS (2016b) Spatial and temporal variations in vegetation cover in an eroded region of subtropical red soil and its relationship with the impact of human activity. *Acta Ecol Sin* 36(21):6960–6968. <https://doi.org/10.5846/stxb201504220831> (in Chinese)
- Xu KJ, Zeng HD, Zhu XB, Tian QJ (2017) Evaluation of five commonly used atmospheric correction algorithms for multi-Temporal aboveground forest carbon storage estimation. *Spectrosc Spectr Anal* 37(11):3493–3498. [https://doi.org/10.3964/j.issn.1000-0593\(2017\)11-3493-06](https://doi.org/10.3964/j.issn.1000-0593(2017)11-3493-06)
- Yan XY, Chen ZQ, Chen ZB, Ma LX (2015) Plant diversity during recovery process of vegetation in eroded red soil region, south China. *J Fujian Norm Univ* 31(2):90–95 (in Chinese)
- Yang YS, Guo JF, Chen GS, Xie JS, Gao R, Li Z et al (2005a) Litter production, seasonal pattern and nutrient return in seven natural forests compared with a plantation in southern China. *Forestry* 78(4):403–415. <https://doi.org/10.1007/s13233-015-3053-x> (in Chinese)
- Yang X, Zhong B, Xie X (2005b) Soil erosion and conservation in red-soil hill area. China Agricultural Press, Beijing (in Chinese)
- Yang Y, Wang L, Yang Z, Xu C, Xie J, Chen G et al (2018) Large ecosystem service benefits of assisted natural regeneration. *J Geophys Res-Biogeosci* 123(2):676–687. <https://doi.org/10.1002/2017JG004267>
- Zeng HD, Xu HQ, Xie JS, Huang SL, Chen WH (2014) Selection of vegetation indices for estimating carbon storage of *Pinus massoniana* forest in a reddish soil erosion region: a case study in Hetian area of Changting county, Fujian Province, China. *Sci Geogr Sin* 34(7):870–875. <https://doi.org/10.13249/j.cnki.sgs.2014.07.870> (in Chinese)
- Zhang Z (2006) Review of the 10th five-year plan and perspective on the 11th five-year plan in relation to natural forest conservation program. *For Eco* 1:49–52 (in Chinese)
- Zhang X, Wang M, Liang X (2009) Quantitative classification and carbon density of the forest vegetation in Lüliang Mountains of China. *Plant Ecol* 201:1–9. <https://doi.org/10.2307/40305617>
- Zhang MY, Wang KL, Liu HY, Zhang CH, Duan YF (2013) Spatio-temporal variation of vegetation carbon storage and density in Karst areas of northwest Guangxi based on remote sensing images. *Chin J Eco-Agric* 21(12):1545–1553. <https://doi.org/10.5814/j.issn.1674-764x.2015.04.002>
- Zhao M, Zhou GS (2006) Carbon storage of forest vegetation in China and its relationship with climatic factors. *Clim Chang* 74:175–189. <https://doi.org/10.1007/s10584-006-6775-0>
- Zhao QG, Zhou SL, Wu SH (2006) Cultivated land resources and strategies for its sustainable utilization and protection in China. *Acta Pedol Sin* 43(4):662–672. <https://doi.org/10.3321/j.issn:0564-3929.2006.04.020> (in Chinese)
- Zhao G, Wu X, Wen Z, Wang F, Gao P (2013) Soil erosion, conservation, and eco-environment changes in the Loess Plateau of China. *Land Degrad Dev* 24:499–510. <https://doi.org/10.1002/ldr.2246>
- Zhao MW, Yue TX, Zhao N, Sun XF, Zhang XY (2014) Combining LPJ-GUESS and HASM to simulate the spatial distribution of forest vegetation carbon stock in China. *J Geogr Sci* 24(2):249–268. <https://doi.org/10.1007/s11442-014-1086-2>
- Zhao J, Guo F, Liang H, Zhangwen SU, Wang W, Lin Y (2016) Changes in temperature and precipitation in Changting, Fujian province during 1965–2013. *J Fujian Agric For Univ* 45(1):77–83. [https://doi.org/10.13323/j.cnki.j.fafu\(nat.sci.\).2016.01.013](https://doi.org/10.13323/j.cnki.j.fafu(nat.sci.).2016.01.013) (in Chinese)
- Zhu HJ (2013) Strategies on eco-restoration in the subtropical mountain ecosystem fragility areas, China: based on the achievement of eleven years' research in Changting county. *J Nat Resour* 28(9):1498–1506. <https://doi.org/10.5814/j.issn.1674-764x.2015.03.002>

Publisher's Note Springer Nature remains neutral with regard to jurisdictional claims in published maps and institutional affiliations.